

# Drying of Films Formed by Ordered Poly(ethylene oxide)–Poly(propylene oxide) Block Copolymer Gels

Zhiyong Gu and Paschalis Alexandridis\*

Department of Chemical and Biological Engineering, University at Buffalo,  
The State University of New York, Buffalo, New York 14260-4200

Received February 24, 2004. In Final Form: September 11, 2004

The drying of hydrogel films formed by poly(ethylene oxide)–poly(propylene oxide) (PEO–PPO) block copolymers (Pluronic P105 and Pluronic L64) is investigated at various air relative humidity (RH) conditions in the range 11–94%. These amphiphilic block copolymers self-assemble to form a variety of ordered (lyotropic liquid crystalline) structures as the water content decreases. The amount of water lost increases linearly with the drying time initially (constant rate region, stage I). After this linear region, a falling rate is observed (stage II). The drying rate increases with decreasing RH, thus greatly shortening the drying time. A decrease of the initial film thickness or a decrease in the initial water content shortens the drying time; however, the drying mechanism remains the same. Analysis of the experimental data shows that the hydration level in the Pluronic hydrogel mainly determines the drying rate, rather than the type of ordered structure formed. Two distinct regions (liquid/gel and solid/crystalline) are observed in the drying isotherm for PEO–PPO block copolymers and homopolymer poly(ethylene glycol)s. A model for one-dimensional water diffusion is used to fit the experimental drying results at different RH, initial film thickness, and initial water content conditions. The model accounts for the shrinkage of the film during drying and for a water diffusion coefficient that is a function of the water concentration in the film. For the experimental conditions considered here, the Biot number ( $Bi$ ) is less than unity and the drying is mainly limited by evaporation at the film surface. The diffusion model is used to obtain information for cases where  $Bi > 1$ .

## Introduction

Film formation is frequently encountered in polymer solution and/or gel applications, e.g., casting of polymer films,<sup>1–4</sup> paints and coatings,<sup>5–12</sup> papers and inks,<sup>12,13</sup> surface cleaning solutions, metal-cutting fluids, foods,<sup>14</sup> cosmetic emulsions and gels applied to skin,<sup>15</sup> and

hydrogels applied to biosurfaces.<sup>16–18</sup> The removal of solvent from polymer solutions and/or gels (drying) is important for the understanding of the film formation process.<sup>8,11</sup> Solvent removal may alter the structure of polymers, for example, from random coils to crystalline or liquid crystalline.<sup>19–22</sup>

Few studies exist on the drying of crystalline (semicrystalline) polymers or gels with ordered structures,<sup>19–22</sup> despite several studies on the drying of disordered polymer solutions.<sup>23–30</sup> The degree of crystallinity of semicrystalline

\* To whom correspondence should be addressed. E-mail: palexand@eng.buffalo.edu. Fax: (716) 645-3822.

(1) Bodmeier, R.; Paeratakul, O. Evaluation of Drug-Containing Polymer Films Prepared from Aqueous Latexes. *Pharm. Res.* **1989**, *6*, 725–730.

(2) *Aqueous Polymeric Coatings for Pharmaceutical Applications*; McGinity, J. W., Ed.; Marcel Dekker: New York, 1989.

(3) Powers, G. W.; Collier, J. R. Experimental Modeling of Solvent-Casting Thin Polymer Films. *Polym. Eng. Sci.* **1990**, *30*, 118–123.

(4) Lippold, B. C.; Pages, R. M. Film Formation, Reproducibility of Production and Curing with Respect to Release Stability of Functional Coatings from Aqueous Polymer Dispersions. *Pharmazie* **2001**, *56*, 5–17.

(5) Blandin, H. P.; David, J. C.; Vergnaud, J. M.; Illien, J. P.; Malizewicz, M. Modeling of Drying of Coatings: Effect of the Thickness, Temperature and Concentration of Solvent. *Prog. Org. Coat.* **1987**, *15*, 163–172.

(6) Croll, S. G. Drying of Latex Paint. *J. Coat. Technol.* **1986**, *58*, 41–49.

(7) Croll, S. G. Heat and Mass Transfer in Latex Paints During Drying. *J. Coat. Technol.* **1987**, *59*, 81–92.

(8) Keddie, J. L. Film Formation of Latex. *Mater. Sci. Eng.* **1997**, *21*, 101–170.

(9) Saure, R.; Wagner, G. R.; Schlunder, E. U. Drying of Solvent-borne Polymeric Coatings: I. Modeling the Drying Process. *Surf. Coat. Technol.* **1998**, *99*, 253–256.

(10) Saure, R.; Wagner, G. R.; Schlunder, E. U. Drying of Solvent-borne Polymeric Coatings: II. Experimental Results Using FTIR Spectroscopy. *Surf. Coat. Technol.* **1998**, *99*, 257–265.

(11) Steward, P. A.; Hearn, J.; Wilkinson, M. C. An Overview of Polymer Latex Film Formation and Properties. *Adv. Colloid Interface Sci.* **2000**, *86*, 195–267.

(12) Guigner, D.; Fischer, C.; Holl, Y. Film Formation from Concentrated Reactive Silicone Emulsions. 1. Drying Mechanism. *Langmuir* **2001**, *17*, 3598–3606.

(13) Avci, A.; Can, M. The Analysis of the Drying Process on Unsteady Forced Convection in Thin Films of Inks. *Appl. Therm. Eng.* **1999**, *19*, 641–657.

(14) Smith, J. S.; Peppas, N. A. Mathematical Analysis of Transport Properties of Polymer Films for Food Packaging. 7. Moisture Transport Through a Polymer Film with Subsequent Adsorption and Diffusion Through Food. *J. Appl. Polym. Sci.* **1991**, *43*, 1219–1225.

(15) Friberg, S. E.; Kayali, I. Water Evaporation Rates from a Model of Stratum Corneum Lipids. *J. Pharm. Sci.* **1989**, *78*, 639–643.

(16) Peppas, N. A.; Hansen, P. J.; Buri, P. A. A Theory of Molecular-Diffusion in the Intestinal Mucus. *Int. J. Pharm.* **1984**, *20*, 107–118.

(17) Larhed, A. W.; Artursson, P.; Grasjo, J.; Bjork, E. Diffusion of Drugs in Native and Purified Gastrointestinal Mucus. *J. Pharm. Sci.* **1997**, *86*, 660–665.

(18) Khanvilkar, K.; Donovan, M. D.; Flanagan, D. R. Drug Transfer through Mucus. *Adv. Drug Delivery Rev.* **2001**, *48*, 173–193.

(19) Ngui, M. O.; Mallapragada, S. Understanding Isothermal Semicrystalline Polymer Drying: Mathematical Models and Experimental Characterization. *J. Polym. Sci., Part B: Polym. Phys.* **1998**, *36*, 2771–2780.

(20) Ngui, M. O.; Mallapragada, S. Mechanistic Investigation of Drying Regimes during Solvent Removal from Poly(vinyl alcohol) Films. *J. Appl. Polym. Sci.* **1999**, *72*, 1913–1920.

(21) Ngui, M. O.; Mallapragada, S. Quantitative Analysis of Crystallization and Skin Formation during Isothermal Solvent Removal from Semicrystalline Polymers. *Polymer* **1999**, *40*, 5393–5400.

(22) Beverley, K. J.; Clint, J. H.; Fletcher, P. D. I. Evaporation Rates of Structured and Non-Structured Liquid Mixtures. *Phys. Chem. Chem. Phys.* **2000**, *2*, 4173–4177.

(23) Okazaki, M.; Shioda, K.; Masuda, K.; Toei, R. Drying Mechanism of Coated Film of Polymer Solution. *J. Chem. Eng. Jpn.* **1974**, *7*, 99–105.

(24) Vergnaud, J. M. *Drying of Polymeric and Solid Materials. Modeling and Industrial Applications*; Springer-Verlag: Germany, 1992.

(25) Lee, M. C.; Peppas, N. A. Water Transport in Epoxy-Resins. *Prog. Polym. Sci.* **1993**, *18*, 947–961.

poly(vinyl alcohol) (PVA) increased during the drying process, and the presence of crystalline structure lowered the drying rate by a factor of as much as 10.<sup>19–21</sup> The development of concentration gradients in ordered structures formed during water evaporation from a nonionic surfactant (*n*-dodecylhexaoxyethylene glycol ether C<sub>12</sub>E<sub>6</sub>)–water system could reduce the water evaporation rate by up to 10 times compared to the values obtained from a simple model that assumed that water transfer in a stagnant vapor layer close to the liquid phase is the limiting step in the water evaporation process.<sup>22</sup>

Pluronic or Poloxamer poly(ethylene oxide)-*block*-poly(propylene oxide)-*block*-poly(ethylene oxide) (PEO-PPO-PEO) copolymers exhibit a variety of ordered (lyotropic liquid crystalline) nanostructures in water (selective solvent for PEO), such as micellar cubic phase, hexagonal phase, bicontinuous cubic phase, and lamellar phase.<sup>31,32</sup> They find numerous applications in coatings and personal care formulations, and also in the area of biomaterials and drug delivery.<sup>33–37</sup> Many of their applications involve the transport of solvent (water) in the block copolymer solutions and/or gels. We are interested in the thermodynamic and transport properties of solvated block copolymers that self-assemble to form ordered structures.<sup>38–40</sup> The ordered structure can undergo a transition from micellar cubic (spherical structural elements arranged in a cubic lattice) to hexagonal (cylinders arranged in a hexagonal lattice) and to lamellar as the water concentration in a PEO-PPO-PEO block copolymer hydrogel decreases.<sup>41</sup> Crystallization of the PEO blocks of the copolymers may occur when the water concentration

is very low.<sup>31</sup> These ordered structures may affect the drying mechanism of such hydrogels.

We report here experimental data on the time evolution of water loss from PEO-PPO-PEO block copolymer hydrogels when brought in contact with air of different relative humidities. The block copolymers considered here, Pluronic P105 and L64, are representative of this class of amphiphilic polymers and form a variety of ordered structures in water.<sup>31</sup> The data allow us to access whether it is the ordered structure formed by block copolymers or the solvation level in the hydrogel that primarily affects the drying rate. The experimental data are fitted to a diffusion model that accounts for film shrinkage and a variable diffusion coefficient. Values for the water diffusion coefficient and the proportionality constant present in the boundary condition at the film–air interface are obtained and discussed. Finally, the effects of initial film thickness, initial water content, Biot number, airflow velocity, and temperature on the drying of PEO-PPO-PEO block copolymer hydrogel films are explored. Our studies not only improve the understanding of formation and drying of films based on amphiphilic block copolymer hydrogels but are also relevant to other applications of surfactant films such as surface cleaning and skin creams.

## Materials and Methods

**Materials.** The Pluronic P105 and Pluronic L64 poly(ethylene oxide)-*block*-poly(propylene oxide)-*block*-poly(ethylene oxide) copolymers were obtained from BASF Corp. and were used as received. Pluronic P105 has a nominal molecular weight of 6500 g/mol and 50 wt % PEO; Pluronic L64 has a nominal molecular weight of 2900 g/mol and 40 wt % PEO. On the basis of their molecular weight and chemical composition, Pluronic P105 and Pluronic L64 can be represented by the formulas (EO)<sub>37</sub>(PO)<sub>58</sub>-(EO)<sub>37</sub> and (EO)<sub>13</sub>(PO)<sub>30</sub>(EO)<sub>13</sub>, respectively. Analytical grade lithium chloride (LiCl), sodium iodide (NaI), sodium bromide (NaBr), sodium chloride (NaCl), potassium chloride (KCl), and potassium nitrite (KNO<sub>2</sub>) were purchased from Fisher Scientific. Saturated aqueous salt solutions were prepared by dissolving an excess amount of salt in water. Millipore-filtered water was used for all sample preparations.

**Generation of Known Constant Water Vapor Pressure.** The driving force for the transfer of solvent (water) from one phase to another is the difference in the solvent chemical potential (or equivalently, osmotic pressure) between the different phases. In our study, the water chemical potential at each air relative humidity (RH) condition examined is more negative than the water chemical potential in the initial hydrogel sample (30 wt % block copolymer or lower), and thus drying is achieved. Equilibrium is attained when the water chemical potentials in each phase become equal to each other. The water chemical potential in the air,  $\Delta\mu$ , can be determined from

$$\Delta\mu = RT \ln\left(\frac{p}{p_0}\right) = RT \ln\left(\frac{\text{RH}}{100}\right) \quad (1)$$

where RH is defined as the water vapor pressure  $p$  divided by the saturated water vapor pressure  $p_0$  (at the same temperature,  $T$ ) and then multiplied by 100. Known water vapor pressures have been generated by saturated aqueous salt solutions<sup>42</sup> as shown in Table 1. Hydrogel samples were placed in a chamber containing air of constant RH (maintained by saturated aqueous salt solutions), and their weight was monitored as a function of time. Experimental details are presented elsewhere.<sup>43</sup> The air

(26) Vrentas, J. S.; Vrentas, C. M. Drying of Solvent-Coated Polymer Films. *J. Polym. Sci., Part B: Polym. Phys.* **1994**, *32*, 187–194.

(27) Cairncross, R. A.; Jeyadev, S.; Dunham, R. F.; Evans, K.; Francis, L. F.; Scriven, L. E. Modeling and Design of an Industrial Dryer with Convective and Radiant Heating. *J. Appl. Polym. Sci.* **1995**, *58*, 1279–1290.

(28) Errede, L. A.; Henrich, P. J. Polymer Drying. 11. Desorption Studies Using Poly-(Styrene-*co*-divinylbenzene) Samples that had been Swelled to Saturation in Chloromethanes. *Adv. Colloid Interface Sci.* **1996**, *66*, 65–161.

(29) Alsoy, A.; Duda, J. L. Modeling of Multilayer Drying of Polymer Films. *J. Polym. Sci., Part B: Polym. Phys.* **1999**, *37*, 1665–1675.

(30) Romdhane, I. H.; Price, P. E.; Miller, C. A.; Benson, P. T.; Wang, S. Drying of Glassy Polymer Films. *Ind. Eng. Chem. Res.* **2001**, *40*, 3065–3075.

(31) Alexandridis, P.; Zhou, D.; Khan, A. Lyotropic Liquid Crystallinity in Amphiphilic Block Copolymers: Temperature Effects on Phase Behavior and Structure of Poly(ethylene oxide)-*b*-Poly(propylene oxide)-*b*-Poly(ethylene oxide) Copolymers of Different Compositions. *Langmuir* **1996**, *12*, 2690–2700.

(32) Alexandridis, P.; Spontak, R. J. Solvent-Regulated Ordering in Block Copolymers. *Curr. Opin. Colloid Interface Sci.* **1999**, *4*, 130–139.

(33) Alexandridis, P. Amphiphilic Copolymers and their Applications. *Curr. Opin. Colloid Interface Sci.* **1996**, *1*, 490–501.

(34) *Amphiphilic Block Copolymers: Self-Assembly and Applications*; Alexandridis, P., Lindman, B., Eds.; Elsevier Science B.V.: Amsterdam, 2000.

(35) Yang, L.; Alexandridis, P. Physicochemical Aspects of Drug Delivery and Release from Polymer-Based Colloids. *Curr. Opin. Colloid Interface Sci.* **2000**, *5*, 132–143.

(36) Kabanov, A. V.; Alakhov, V. Y. Pluronic (R) Block Copolymers in Drug Delivery: From Micellar Nanocontainers to Biological Response Modifiers. *Crit. Rev. Ther. Drug* **2002**, *19*, 1–72.

(37) Bromberg, L.; Temchenko, M.; Hatton, T. A. Smart Microgel Studies. Polyelectrolyte and Drug-Absorbing Properties of Microgels from Polyether-Modified Poly(acrylic acid). *Langmuir* **2003**, *19*, 8675–8684.

(38) Alexandridis, P.; Gu, Z. Equilibrium Swelling and Drying Kinetics of Poloxamer Hydrogel Films. *Polym. Prepr. (Am. Chem. Soc., Div. Polym. Chem.)* **2002**, *43*, 627–628.

(39) Gu, Z.; Alexandridis, P. Water Activity in Polyoxyethylene-*b*-Polyoxypropylene (Poloxamer) Aqueous Solutions and Gels. *Polym. Mater. Sci. Eng.* **2003**, *89*, 238–239.

(40) Gu, Z.; Alexandridis, P. Osmotic Stress Measurements of Intermolecular Forces in Ordered Assemblies Formed by Solvated Block Copolymers. *Macromolecules* **2004**, *37*, 912–924.

(41) Yang, L.; Alexandridis, P. Mass Transport in Ordered Microstructures Formed by Block Copolymers: Ramifications for Controlled Release Applications. *Polym. Prepr. (Am. Chem. Soc., Div. Polym. Chem.)* **1999**, *40*, 349–350.

(42) Greenspan, L. Humidity Fixed Points of Binary Saturated Aqueous Solutions. *J. Res. Natl. Bur. Stand. A: Phys. Chem.* **1977**, *81A*, 89–96.

(43) Gu, Z.; Alexandridis, P. Drying of Poloxamer Hydrogel Films. *J. Pharm. Sci.* **2004**, *93*, 1454–1470.

**Table 1. Relative Humidity (RH) and Water Chemical Potential ( $\Delta\mu$ ) of Saturated Aqueous Salt Solutions at 24 °C**

salt	LiCl	NaI	NaBr	NaCl	KCl	KNO <sub>3</sub>
RH <sup>a</sup>	11.3	38.5	57.9	75.4	84.6	93.8
$\pi$ , atm	2951	1295	740	383	226	86
$\Delta\mu$ , J/mol	-5382	-2361	-1350	-699	-413	-157

<sup>a</sup> These values are interpolated from ref 42, where the RH of saturated salt solutions is reported as a function of temperature. For simplicity, 11.3% RH is written as 11% RH in the following text and figures; similar simplifications are made for other RH conditions.

was still, and the air velocity was not a variable over our drying experiments. The total time required for the drying of Pluronic P105 hydrogel ranged from about 12 days for relatively dry air conditions (11% RH) to about 42 days for relatively humid air conditions (94% RH) when the initial film thickness was 5 mm and the initial block copolymer concentration was 30 wt %.

The Pluronic block copolymer concentration and water loss as a function of time data reported in Results and Discussion are the average values of two sets of experiments, conducted in parallel at the same temperature and same RH. Very good reproducibility was observed: the errors were generally below 1% (the maximum error was 4%), and the error bars are smaller than the symbols used in the figures.

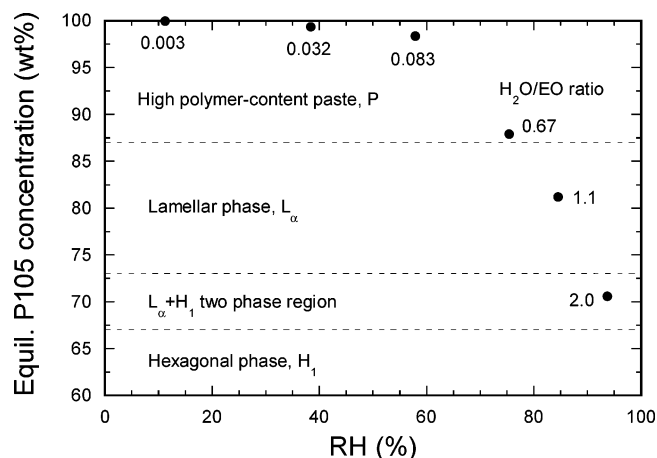
**Hydrogel Film Formation.** To prepare the 10 and 20 wt % Pluronic P105 aqueous solutions, the block copolymer was mixed with water until a homogeneous solution was obtained. To prepare the 30 wt % Pluronic P105 hydrogel, the block copolymer was mixed with water and kept in a refrigerator (4 °C) for several days until a homogeneous solution was obtained. Upon a slow increase in temperature, a phase transition occurred from the micellar solution to the micellar cubic liquid crystalline phase,<sup>31</sup> and a uniform and smooth film of transparent hydrogel was formed. In the case of Pluronic L64, the initial concentration (30 wt %) corresponds to an isotropic (micellar) solution.<sup>44</sup>

We examined films of three different initial thicknesses (1, 3, and 5 mm) in order to access the effect of film thickness on the drying course of Pluronic P105 hydrogels. The 5 mm film thickness was used for all the air RH conditions, while 1 and 3 mm films were examined at 58% and 85% RH. Different initial water contents (10, 20, and 30 wt % Pluronic P105) were also examined at 58% RH. The film surface receded toward the bottom of the container during the drying process. When the water content in the Pluronic P105 hydrogel was low (about 10–20 wt % H<sub>2</sub>O), the sample became opaque because of semicrystalline domains formed by the poly(ethylene oxide) blocks. This change in appearance coincides with the phase boundary between the lamellar phase and the high-polymer-content paste phase.<sup>31</sup> At this point, the film surface was no longer smooth but developed some wrinkles. The Pluronic L64 samples remained transparent and had smooth surfaces throughout the drying process.

## Results and Discussion

**Equilibrium Water Content.** The equilibrium concentrations of PEO–PPO–PEO block copolymer hydrogels are different depending on the RH (see Figure 1) and correspond to different ordered structures.<sup>40</sup> The dotted lines in Figure 1 indicate the phase boundaries at different compositions.<sup>31</sup> Table 2 lists the equilibrium concentration and the hydration level (H<sub>2</sub>O/EO molar ratio) of PEO–PPO–PEO block copolymer hydrogels at different RH values. These values are very relevant to the drying experiments because they correspond to the infinite time conditions.

During the drying process, various ordered structures form. In the case of Pluronic P105, the micellar cubic, hexagonal, and lamellar lyotropic liquid crystalline phases

**Figure 1.** Equilibrium concentration (wt %) of Pluronic P105 in the hydrogel film plotted as a function of the relative humidity (RH) in the air. The values next to the data points indicate the water/EO molar ratio at equilibrium. The dotted lines indicate the block copolymer concentration where the ordered structure changes.**Table 2. Equilibrium Concentration of Pluronic P105 and Pluronic L64 in the Hydrogel and Hydration Numbers (Moles Water per EO Segment) at Different RH Conditions**

Pluronic P105						
	RH (%)					
	11	38	58	75	85	94
P105 wt %	99.94	99.34	98.33	87.91	81.16	70.55
H <sub>2</sub> O/EO ratio	0.003	0.032	0.083	0.67	1.1	2.0
Pluronic L64						
	RH (%)					
			58	85		
L64 wt %			97.03	86.48		
H <sub>2</sub> O/EO ratio			0.19	0.96		

will successively form during the drying course when the initial concentration of the hydrogel sample is 30 wt %. At low RH conditions ( $\leq 58\%$ ), the block copolymer hydrogel retains very low water content at equilibrium ( $\leq 2$  wt %) and thus contains crystalline PEO (as attested by the opacity of the film). For example, when the RH is 58%, the water content is about 1.7 wt % (H<sub>2</sub>O/EO molar ratio = 0.083, corresponding to the high-polymer-content paste region in the phase diagram). When the RH increases to 85% or higher, the equilibrium water content in the Pluronic P105 hydrogel increases accordingly (see Table 2). For example, at 85% RH, the H<sub>2</sub>O/EO molar ratio is 1.1 and the Pluronic P105 concentration 81.2 wt % (corresponding to the lamellar phase).

In the case of Pluronic L64, the hexagonal, lamellar liquid crystalline, and high-polymer-content solution phases will successively form during the drying process when the initial block copolymer concentration is 30 wt %. Because pure Pluronic L64 is liquid (melt) and the equilibrium concentrations in the air RH conditions studied (58–85% RH) fall in the high-polymer-content solution region,<sup>44</sup> the final film formed after the drying process is transparent and liquid (equilibrium concentrations and hydration values can be found in Table 2). However, the equilibrium structure may be lamellar or hexagonal at higher air RH values (corresponding to higher water concentrations in the film).

**Time Evolution of Water Loss.** Figure 2a shows the evolution of the Pluronic P105 concentration as a function of drying time when the initial film thickness is 5 mm and

(44) Alexandridis, P.; Olsson, U.; Lindman, B. Self-Assembly of Amphiphilic Block Copolymers: The (EO)<sub>13</sub>(PO)<sub>30</sub>(EO)<sub>13</sub>-Water-*p*-Xylene System. *Macromolecules* **1995**, *28*, 7700–7710.



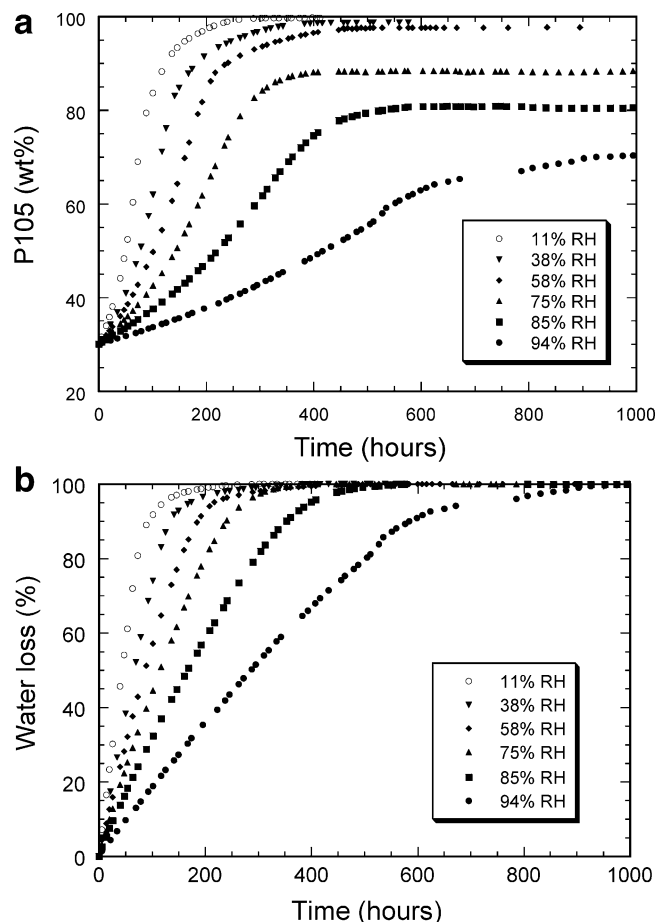


**Figure 2.** (a) Pluronic P105 block copolymer concentration (wt %) in the hydrogel film vs drying time at different RH values (indicated in the figure). (b) Percentage of water loss vs drying time at different RH values.

the initial block copolymer concentration is 30 wt %. The concentration reported in Figure 2a is the average concentration over the whole film and is calculated on the basis of a mass balance at any given time. The percentage of water loss (defined as water weight loss at time  $t$  divided by water weight loss at infinite time) from the film initially increases linearly with the drying time; after this linear region (constant rate region, stage I), a nonlinear behavior is observed (falling rate region, stage II, see Figure 2b) leading to a plateau. Higher RH increased the time needed for the water weight loss, but in all the air RH conditions examined, the percentage of water loss increased linearly with the time initially. The linear region and nonlinear region in the water loss vs time curves (Figure 2b) follow the two-stage mechanism for the drying process observed by many researchers.<sup>6-8,10,11,45-48</sup> Although the polymer entanglement and strong hydration present in the block copolymer hydrogels will hinder the water transport in the hydrogel,<sup>49-51</sup> the water content in the hydrogel is very high initially (70 wt % H<sub>2</sub>O) and water can move relatively freely. So the drying process in stage I is limited

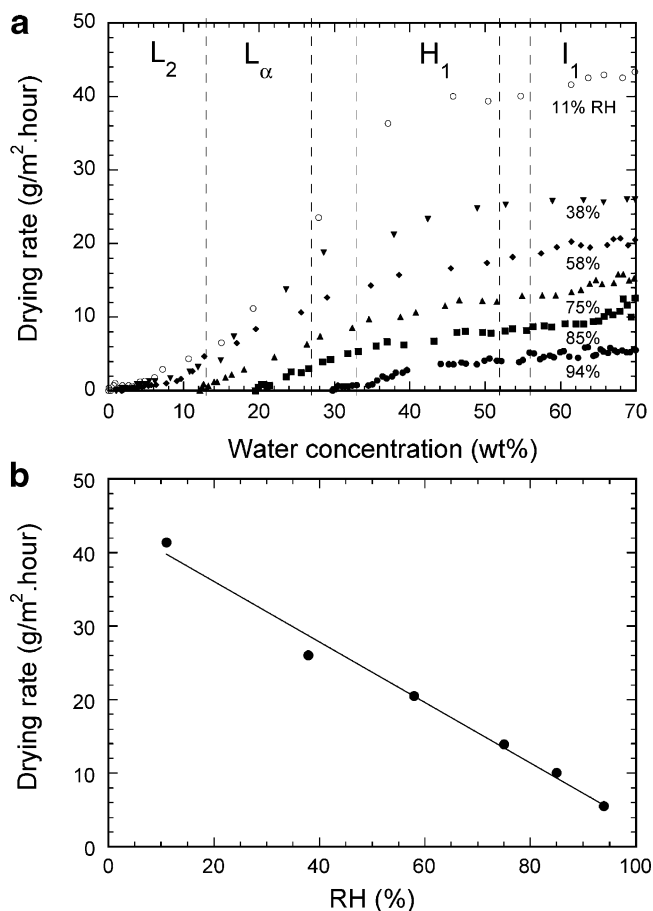


**Figure 3.** (a) Drying rate vs water content at different RH values for Pluronic P105 hydrogels. (b) Drying rate at stage I as a function of RH. The dotted lines in panel a indicate the water concentration where the ordered structure changes. L<sub>1</sub>, micellar solution; I<sub>1</sub>, micellar cubic phase; H<sub>1</sub>, hexagonal phase; L<sub>α</sub>, lamellar phase; L<sub>2</sub>, high-polymer-content paste. RH: ○, 11%; ▼, 38%; ◆, 58%; ▲, 75%; ■, 85%; ●, 94%.

by the water evaporation at the film surface. When the time proceeds and the water concentration becomes low, polymer structure (entanglement or crystallinity) and hydration are expected to play a more important role, and both surface evaporation and water transport in the structured hydrogel will affect the drying rate. This corresponds to stage II of drying.

The drying rate, i.e., the derivative of the water loss with respect to time (Figure 2b), is plotted in Figure 3a as a function of water concentration in the film (corresponding to the time when a particular drying rate is calculated). For all the air RH conditions considered here, as described before, the drying rate is constant at high water contents (stage I), followed by a falling rate region (stage II). The drying rate in stage I of the drying process decreases linearly with an increase of the air RH (Figure 3b). The drying rate at stage I is 41.4 g/(m<sup>2</sup> h) at 11% RH (when the initial film thickness is 5 mm and the initial block copolymer concentration 30 wt %), but when RH increases to 94%, the drying rate drops to 5.5 g/(m<sup>2</sup> h), about an 8-fold decrease. The time duration of the constant

(45) Scherer, G. M. Aging and Drying of Gels. *J. Non-Cryst. Solids* **1988**, *100*, 77-92.

(46) Gutoff, E. B. The Drying of Waterborne Coatings. *ACS Symp. Ser.* **1997**, *663*, 245-264.

(47) McCabe, W. L.; Smith, J. C.; Harriot, P. *Unit Operations of Chemical Engineering*, 6th ed.; McGraw-Hill: New York, 2001.

(48) Etemad, S. Gh.; Etesami, N.; Bagheri, R.; Thibault, J. Drying of Latex Films of Poly(vinyl acetate). *Drying Technol.* **2002**, *20*, 1843-1854.

(49) Malmsten, M.; Lindman, B. Water Self-Diffusion in Aqueous Block Copolymer Solutions. *Macromolecules* **1992**, *25*, 5446-5450.

(50) Coppola, L.; Oliviero, C.; Pogliani, L.; Ranieri, G. A.; Terenzi, M. A Self-Diffusion Study in Aqueous Solution and Lyotropic Mesophases of Amphiphilic Block Copolymers. *Colloid Polym. Sci.* **2000**, *278*, 434-442.

(51) Borodin, O.; Bedrov, D.; Smith, G. D. Concentration Dependence of Water Dynamics in Poly(Ethylene Oxide)/Water Solutions from Molecular Dynamics Simulations. *J. Phys. Chem. B* **2002**, *106*, 5194-5199.

rate region becomes longer when the RH is higher. At 11% RH, the total drying time is about 290 h when the initial film thickness is 5 mm, but at 94% RH, the total drying time increases to 1000 h (about 42 days).

To compare the stage I drying rate of Pluronic P105 hydrogel to the evaporation of pure water, we dried water films using the same methodology and conditions as the Pluronic films at relative humidities in the range 11–58%. We found the evaporation rate of pure water to be very similar to (or slightly higher than) that of the hydrogel in stage I drying at the same RH conditions. The drying rate of an alumina gel has been observed to be constant in the first stage of drying (when the water content is greater than about 70%) and is almost the same as the evaporation rate of pure water.<sup>45,52</sup> This is similar to our observation for the drying of Pluronic hydrogels at conditions examined above.

Fletcher and co-workers have examined the evaporation rate of water from various media, e.g., pure liquid,<sup>53</sup> emulsions,<sup>54</sup> and structured and nonstructured liquid mixtures.<sup>22</sup> The evaporation rate of pure water at 25 °C reported by Beverley et al.<sup>53</sup> is about 20 times higher than the value obtained in our study at 11% RH and 24 °C. However, whereas the air in our study was kept still, a high gas flow rate (pure nitrogen, gas velocity of about 3.5 cm/s or higher) was employed in ref 53 and such high flow rate can increase the evaporation rate greatly. It has also been indicated that the initial water evaporation rate from pure water is constant at fixed temperature, and the evaporation rate is proportional to the vapor pressure of the sample,<sup>53</sup> similarly to the results obtained in our study in the stage I drying and pure water evaporation. They also observed that in the water-rich compositions of the nonionic surfactant C<sub>12</sub>E<sub>6</sub>–water system (water mole fraction > 0.85, corresponding to >16 wt % water), the water evaporation rates were only slightly smaller than the values predicted from a simple model which assumed that water transfer in a stagnant vapor layer close to the liquid phase is the limiting step in the water evaporation process, and the concentration gradients in the mixtures are relatively small.<sup>22</sup> This is very similar to the observations in our study, where the drying rate in stage I is only slightly lower than that of pure water, and the drying rate is mainly determined by the water evaporation. Furthermore, the self-assembled structures (including micellar solution, micellar cubic, hexagonal, and lamellar lyotropic liquid crystals) formed by C<sub>12</sub>E<sub>6</sub> only slightly lowered the vapor pressure of the mixture and no large concentration gradient was developed in the water-rich compositions (water mole fraction > 0.85) of the surfactant–water mixture.<sup>22</sup> Interestingly, no large water evaporation rate changes were observed at phase boundaries in the C<sub>12</sub>E<sub>6</sub>–water system,<sup>22</sup> which is consistent with our measurements as shown in Figure 3a.

The drying of Pluronic L64 hydrogel films was conducted at 58% and 85% RH conditions, and the water loss per area vs drying time data are shown in Figure 4a (the initial film thickness is 3 mm for both conditions). Similar to the drying of Pluronic P105 hydrogels, two stages were observed for Pluronic L64. In stage I, water loss per area is a linear function of the drying time and the drying rate is constant; while in stage II, the drying rate falls. The

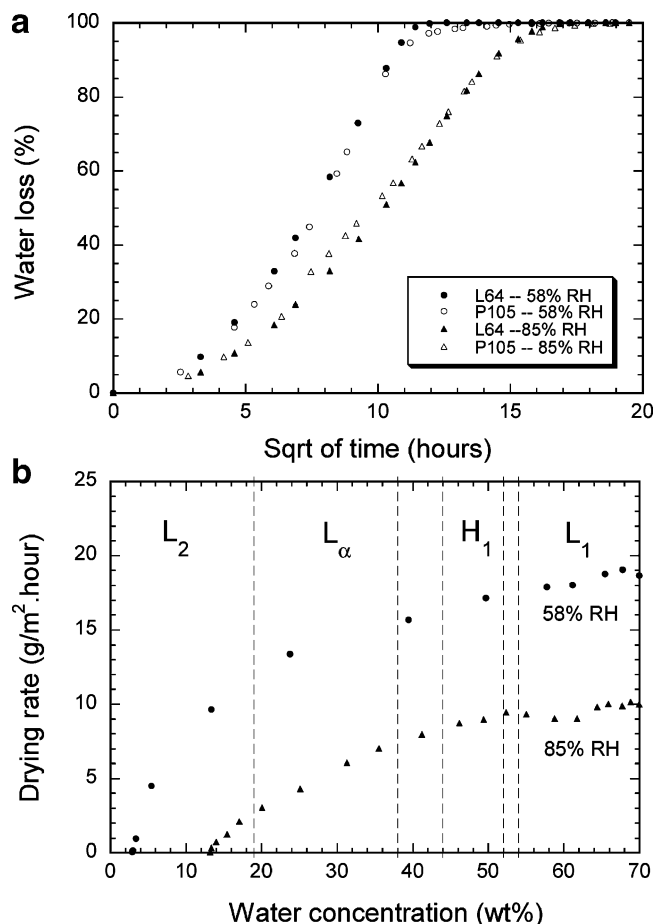


**Figure 4.** (a) Water loss per unit area vs square root of drying time and (b) drying rate vs water content for Pluronic L64 at 58% and 85% RH values. The dotted lines in panel b indicate the water concentration where the ordered structure changes. The notation for the different phases is the same as in Figure 3.

drying rate vs water content data are shown in Figure 4b. In the micellar solution (L<sub>1</sub>) and hexagonal phase (H<sub>1</sub>), the drying rate is relatively constant; while in the lamellar phase (L<sub>α</sub>) and the high-polymer-content phase (L<sub>2</sub>), the drying rate drops greatly for both air RH conditions considered. Note that the vertical dotted lines in this figure (also in Figure 3a) indicate the equilibrium water concentration at which the self-assembled structure undergoes a phase transition. For the block copolymer–selective solvent systems considered here which self-assemble in a reversible, dynamic manner,<sup>55,56</sup> the dynamics of phase transitions is usually faster than the diffusion time scale (here, on the order of weeks); we can thus consider the internal structure at a given concentration (during the drying process) to correspond to the structure expected at equilibrium.

**What Determines the Drying Rate: Ordered Structure or Hydration Level?** It has been reported that gas permeability or molecular diffusion are affected by the complex or ordered structures formed by block copolymers.<sup>57–61</sup> For example, gas permeability in poly-

(52) Dwivedi, R. K. Drying Behavior of Alumina Gels. *J. Mater. Sci. Lett.* **1986**, *5*, 373–376.

(53) Beverley, K. J.; Clint, J. H.; Fletcher, P. D. I. Evaporation Rates of Pure Liquids Measured Using a Gravimetric Technique. *Phys. Chem. Chem. Phys.* **1999**, *1*, 149–153.

(54) Aranberri, I.; Beverley, K. J.; Binks, B. P.; Clint, J. H.; Fletcher, P. D. I. How Do Emulsions Evaporate? *Langmuir* **2002**, *18*, 3471–3475.

(55) Kositzka, M. J.; Bohne, C.; Alexandridis, P.; Hatton, T. A.; Holzwarth, J. F. Dynamics of Micro- and Macrophase Separation of Amphiphilic Block-Copolymers in Aqueous Solution. *Macromolecules* **1999**, *32*, 5539–5551.

(56) Zipfel, J.; Berghausen, J.; Schmidt, G.; Lindner, P.; Alexandridis, P.; Richtering, W. Influence of Shear on Solvated Amphiphilic Block Copolymers with Lamellar Morphology. *Macromolecules* **2002**, *35*, 4064–4074.

styrene–polybutadiene block copolymer films with oriented lamellar structures depends greatly on the direction of domain orientation: in domains that were oriented normal to the film surface, gas permeability was found to be higher than that in domains that were oriented parallel to the film surface.<sup>57</sup> Semicrystalline structures formed by polyethylene–poly(ethylene–propylene) diblock copolymers had a significant effect on the gas permeability: gas permeability was lower in the crystalline polyethylene domains than in the amorphous poly(ethylene–propylene) domains.<sup>58</sup> The diffusion coefficients of small molecules in polystyrene–polybutadiene–polystyrene block polymers with a lamellar structure have been determined experimentally, and the sorption of small molecules in block copolymers has been described by an unsteady-state model, which assumed that the diffusion in one of the phases (components) of the block copolymer is much faster than in the other phase.<sup>59</sup>

Since complex or ordered structures affect molecular diffusion in polymer systems as indicated above, it may be reasonable to assume that the ordered (self-assembled) structures present in the systems examined here may also affect the drying mechanism and time course. As shown in Figure 3a, the drying rate of Pluronic P105 hydrogels is greatly affected by the water content (correspondingly, the type of ordered structure). For example, the drying rate remains almost the same in the micellar cubic phase and the first half of the hexagonal phase (water concentration above 44 wt %, corresponding to the stage I drying) at all the RH conditions examined. However, the drying rate drops greatly in the second half of the hexagonal phase and in the lamellar phase region, and also in the high-polymer-content semicrystalline paste region. This corresponds to the stage II drying.

The drying behavior of the high-PEO-content (70%) Pluronic F127 ((EO)<sub>100</sub>(PO)<sub>70</sub>(EO)<sub>100</sub>) and homopolymer (100% PEO) poly(ethylene glycol)s (PEGs) of molecular weights 4000 and 20000 has been recently reported.<sup>38,43</sup> This enables a comparison with the intermediate PEO content block copolymers considered here. The drying rate vs water content curves for the different polymers are shown together in Figure 5a,b for 58% and 85% RH, respectively. Initially, the drying rate is relatively constant for all the polymers. However, the drying rate drops with a decrease of the solvent content, and the change of drying rate is different depending on the polymer. The drying rate is lower when the PEO content of the polymer is higher; i.e., the magnitude of the drying rate at the same water content follows the order L64 (40 wt % PEO) > P105 (50 wt % PEO) > F127 (70 wt % PEO) > PEG (100% PEO). For the drying of PEG4000 and PEG20000, the drying rates are very similar to each other at 58% RH and for most of the time course at 85% RH. However, the behavior of the drying rate of PEG20000 at 85% RH and PEG4000 and PEG20000 at 58% RH changed at the later

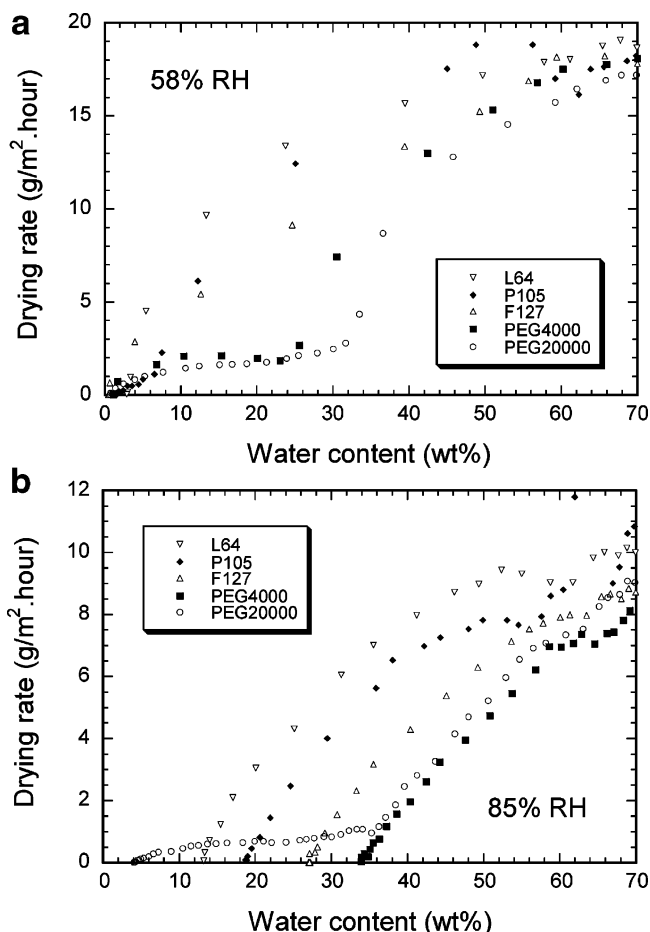


**Figure 5.** Drying rate vs water content curves for different polymers/block copolymers at (a) 58% and (b) 85% RH.

stage of the drying process; this may be due to the development of crystalline structure by PEO.

Since the initial block copolymer concentrations in the Pluronic hydrogels considered here are well above their critical micellization concentration,<sup>62</sup> the basic structural units in the block copolymer hydrogels are micelles. The micelle core consists mainly of hydrophobic PPO, while the micelle corona consists of hydrated PEO.<sup>63</sup> It has been established that the intermolecular interactions in PEO–PPO–PEO block copolymer hydrogels are mainly accounted for by the interactions between PEO and water,<sup>40</sup> so it is reasonable to assume that the diffusion of water in such systems is mainly affected by the interactions between PEO and water. On the basis of this hypothesis, the drying rate vs water content curve was replotted based on the “corrected” water content ( $H_2O$  wt %\*) defined below:

$$H_2O \text{ wt \%}^* = \frac{H_2O \text{ wt \%}}{(100 - H_2O \text{ wt \%}) \times PEO \text{ wt \%} + H_2O \text{ wt \%}} \quad (2)$$

where  $H_2O$  wt % is the water content in the PEO–PPO–PEO block copolymer–water system, and PEO wt % is

(57) Csernica, J.; Baddour, R. F.; Cohen, R. E. Morphological Arrangements of Block Copolymers that Result in Low Gas Permeability. *Macromolecules* **1990**, *23*, 1429–1433.

(58) Kofinas, P.; Cohen, R. E.; Halasa, A. F. Gas Permeability of Polyethylene/Poly(ethylene–propylene) Semicrystalline Diblock Copolymers. *Polymer* **1994**, *35*, 1229–1235.

(59) Faridi, N.; Duda, J. L.; Hadj-Romdhane, I. Unsteady-State Diffusion in Block Copolymers with Lamellar Domains. *Ind. Eng. Chem. Res.* **1995**, *34*, 3556–3567.

(60) Walderhaug, H. PFG NMR Study of Polymer and Solubilize Dynamics in Aqueous Isotropic Mesophases of Some Poloxamers. *J. Phys. Chem. B* **1999**, *103*, 3352–3357.

(61) Chen, B. H.; Miller, C. A.; Walsh, J. M.; Warren, P. B.; Ruddock, J. N.; Garrett, P. R.; Argoul, F.; Leger, C. Dissolution Rates of Pure Nonionic Surfactants. *Langmuir* **2000**, *16*, 5276–5283.

(62) Alexandridis, P.; Holzwarth, J. F.; Hatton, T. A. Micellization of Poly(ethylene oxide)–Poly(propylene oxide)–Poly(ethylene oxide) Triblock Copolymers in Aqueous Solutions: Thermodynamics of Copolymer Association. *Macromolecules* **1994**, *27*, 2414–2425.

(63) Yang, L.; Alexandridis, P.; Steytler, D. C.; Kositz, M. J.; Holzwarth, J. F. SANS Investigation of the Temperature-Dependent Aggregation Behavior of the Block Copolymer Pluronic L64 in Aqueous Solution. *Langmuir* **2000**, *16*, 8555–8561.



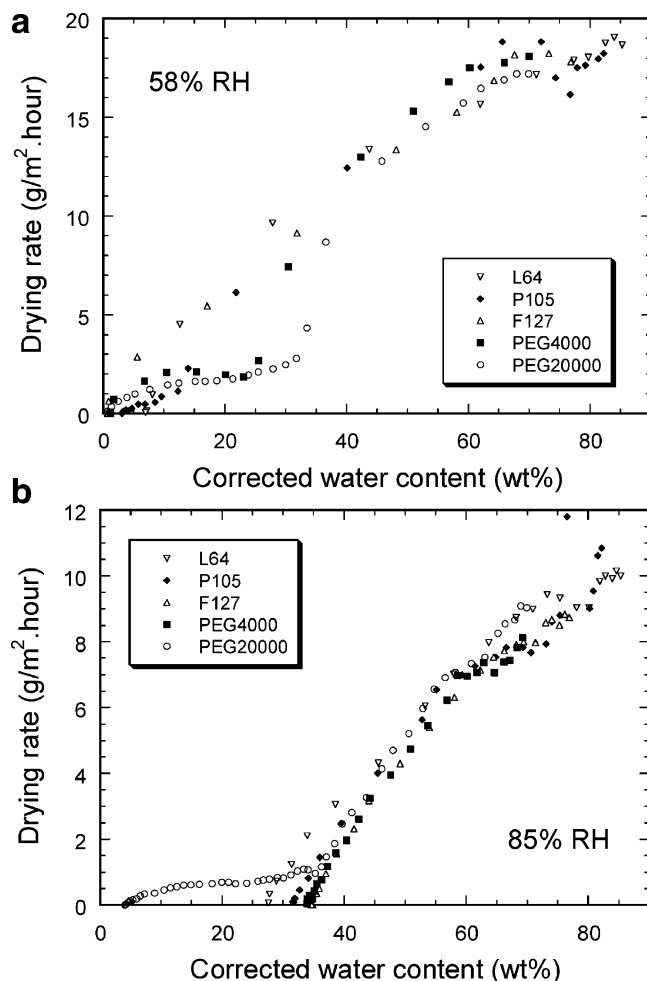


**Figure 6.** Drying rate vs corrected water content ( $\text{H}_2\text{O}$  wt %\*, calculated based on eq 2) curves for different polymers/block copolymers at (a) 58% and (b) 85% RH.

the PEO content of a block copolymer molecule, for example, PEO wt % = 40 for Pluronic L64. The corrected water content aims to capture the hydration level at different block copolymer concentrations. The drying rate vs the corrected water content ( $\text{H}_2\text{O}$  wt %\*) data are shown in Figure 6a,b. When plotted against the corrected water content, the drying rates of different PEO–PPO–PEO block copolymers overlap fairly well in most regions of the drying curves for both 58% and 85% RH conditions. Moreover, the drying rates of Pluronic hydrogels compare very well with these of PEG solutions when the water content is high (when there is no crystallinity). This indicates that the hydration level, rather than the type of ordered structure, plays a more important role in the drying process of Pluronic hydrogels. This is not unexpected since the ordered structures formed by the block copolymers considered here are water-continuous.

The corrected equilibrium water content for all the polymers and block copolymers examined here is plotted in Figure 7 as a function of the air RH. Two different lines (trends) can be discerned: one is the liquid or gel line, where the equilibrium concentrations that fall on this line correspond to liquid (solution) or gel (lyotropic liquid crystal) phases; the other is the crystalline (or semicrystalline) line, where the equilibrium concentrations correspond to semicrystalline states. For example, Pluronic L64 is liquid in the neat form and is liquid or gel when mixed with water; thus the equilibrium concentrations of Pluronic L64 will fall on the liquid/gel line, no matter

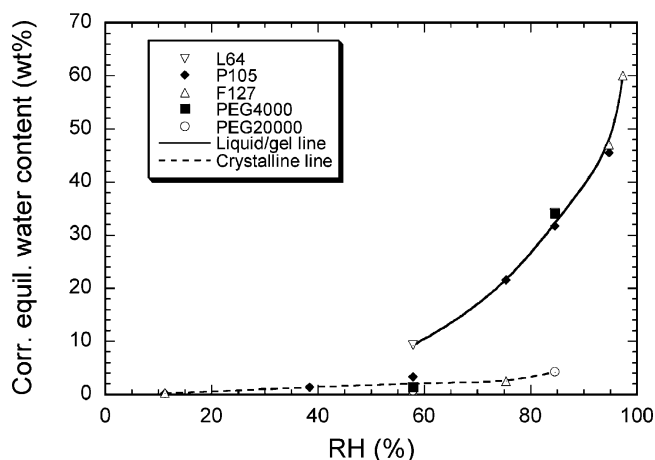


**Figure 7.** Corrected water content as a function of RH for different polymers/block copolymers.

what the RH is. However, for Pluronic F127, when the RH is high ( $\geq 85\%$ ), the equilibrium state is hydrogel and the equilibrium concentrations fall on the liquid/gel line; for  $\text{RH} < 75\%$ , Pluronic F127 is semicrystalline so the equilibrium concentrations will be located on the crystalline line. The features of Figure 7 can be used to correlate qualitatively the water content of PEO–PPO block copolymer or PEO homopolymer systems in equilibrium with water vapor with the polymer microstructure at these conditions. A quantitative model is needed in order to predict the equilibrium concentrations of (solvated) block copolymers at different RH conditions (i.e., solvent chemical potential). Mean field lattice models employed by our group have successfully predicted phase behavior and structure in amphiphilic block copolymer–water (selective solvent) systems.<sup>64,65</sup>

**Water Diffusion in the Hydrogel Film.** Mathematical modeling can be used to fit experimental data and to obtain optimum operating conditions for the drying process. The diffusion of water in the hydrogel film can be described by Fick's second law:<sup>66</sup>

$$\frac{\partial C}{\partial t} = \frac{\partial}{\partial x} \left( D \frac{\partial C}{\partial x} \right) \quad (3)$$

where  $C$  is the concentration of water in the hydrogel,  $\text{g}/\text{m}^3$ ;  $t$  is drying time;  $x$  is the water diffusion direction (normal to the surface of the hydrogel film); and  $D$  is the diffusion coefficient of water in the hydrogel.  $D$  is generally a function of the water concentration and, correspondingly, polymer concentration. In systems with internal order and/or anisotropy, the diffusion coefficient should be a function of the microstructure. Here we do not account for such dependence on the basis of the conclusion (reached in the previous section) regarding the relative importance on drying of hydration (water concentration) over the type of self-assembled structure. Note that eq 3 describes diffusion in one-dimensional geometry. For the experimental setup of our studies,<sup>43</sup> this would mean that we neglect the finite diameter of the cylindrical film specimens and assume lateral homogeneity in the film. This as-

(64) Svensson, M.; Alexandridis, P.; Linse, P. Phase Behavior and Microstructure in Binary Block Copolymer–Selective Solvent Systems: Experiments and Theory. *Macromolecules* **1999**, *32*, 637–645.

(65) Shusharina, N. P.; Balijepalli, S.; Gruenbauer, H. J. M.; Alexandridis, P. Mean-Field Theory Prediction of the Phase Behavior and Phase Structure of Alkyl-Propoxy-Ethoxylate “Graded” Surfactants in Water: Temperature and Electrolyte Effects. *Langmuir* **2003**, *19*, 4483–4492.

(66) Crank, J. *The Mathematics of Diffusion*, 2nd ed.; Clarendon Press: Oxford, U.K., 1975.

sumption is reasonable, given the small ratio of film thickness to film diameter.<sup>43</sup>

Since there is a large water vapor source (large amount of saturated aqueous salt solutions) in the sealed container where we kept the hydrogel film for drying, the water vapor pressure in contact with the Pluronic hydrogel film is considered constant at all times. In the case of variable film thickness (a function of water content in the film), the boundary condition at the film–air interface is obtained by a jump mass balance,<sup>26,29,30,67</sup> where the term  $C(dh(t)/dt)$  accounts for the water flux due to the moving boundary:

$$-D \frac{\partial C}{\partial x} - C \frac{dh(t)}{dt} = k_G(p^G - p_b^G) \quad x = h(t) \quad (4)$$

where  $h(t)$  is the thickness of the hydrogel film and is a function of drying time;  $k_G$  is the mass transfer coefficient between the film surface and the adjacent air;  $p^G$  is the water partial pressure at the film–air interface; and  $p_b^G$  is the water pressure in the bulk air (constant at all times).

The water partial vapor pressure at the film–air interface ( $p^G$ ) is the product of pure water pressure at the same temperature ( $p_0$ ) multiplied by the water activity at the film–air interface. Since the water activity at the film–air interface is usually unknown, an equation of state (EOS) is needed to correlate the water activity with the water concentration (correspondingly, water volume fraction) in the block copolymer phase. The Flory–Huggins theory is widely used to describe the solvent activity in polymer systems<sup>68</sup> and has been utilized in the modeling of drying of polymer solutions.<sup>9,26,29,30,67</sup> However, for the systems examined here, the Flory–Huggins equation is not adequate to describe the water activity.<sup>39</sup> Instead, we used a linear function to correlate the water vapor pressure and water concentration:

$$p = mC \quad (5)$$

where  $m$  is a proportionality constant.

Insertion of eq 5 into eq 4 gives

$$\begin{aligned} -D \frac{\partial C}{\partial x} - C \frac{dh(t)}{dt} &= k_G m (C - C_\infty) \quad x = h(t) \\ &= \alpha (C - C_\infty) \end{aligned} \quad (6)$$

where  $C_\infty$  is the water concentration which is in equilibrium with the air relative humidity;  $\alpha$  is a proportionality constant that represents the product of the mass transfer coefficient  $k_G$  and the proportionality constant  $m$ . Equation 6 is used here as a boundary condition to solve eq 3.

The boundary condition at the bottom of the hydrogel film is

$$D \frac{\partial C}{\partial x} = 0 \quad x = 0 \quad (7)$$

The initial condition is

$$C = C_0 \quad t = 0 \quad x = 0 \rightarrow L_0 \quad (8)$$

where  $C_0$  is the initial water concentration in the hydrogel film and  $L_0$  the initial film thickness.

(67) Price, P. E.; Cairncross, R. A. Optimization of Single-Zone Drying of Polymer Solution Coatings Using Mathematical Modeling. *J. Appl. Polym. Sci.* **2000**, *78*, 149–165.

(68) Flory, P. J. *Principles of Polymer Chemistry*; Cornell University Press: Ithaca, NY, 1953.

The film thickness at different times is obtained by a polymer mass balance in the hydrogel film:

$$h(t) = \frac{L_0(1 - w_{0,H_2O})}{1 - \bar{w}_{H_2O}(t)} = \frac{L_0(1 - w_{0,H_2O})}{1 - \int_0^{h(t)} w_{H_2O}(t) dx} \quad (9)$$

where  $w_{0,H_2O}$  is the initial water weight fraction;  $\bar{w}_{H_2O}(t)$  is the average water weight fraction in the hydrogel film at time  $t$ .

The total quantity of water that has crossed a unit area of the surface by time  $t$ ,  $M(t)$ , is

$$\begin{aligned} M(t) &= L_0 C_0 - h(t) \bar{C}(t) \\ &= L_0 C_0 - h(t) \int_0^{h(t)} C(x,t) dx \end{aligned} \quad (10)$$

The water diffusion coefficient in the hydrogel is taken to be an exponential function of the water concentration:<sup>5,69</sup>

$$D = D_0 e^{-h/C} \quad (11)$$

where  $D_0$  is a pre-exponential factor (it has units of diffusion coefficient), and  $k$  is a constant.

The dimensionless forms of eqs 3 and 6–11 are obtained by using the following dimensionless variables:

$$C^* = \frac{C}{C_0} \quad (12)$$

$$t^* = \frac{L_0^2 t}{D_0} \quad (13)$$

$$x^* = \frac{x}{L_0} \quad (14)$$

$$h^*(t) = \frac{h(t)}{L_0} \quad (15)$$

$$\alpha^* = \frac{\alpha L_0}{D_0} \quad (16)$$

$$D^* = \frac{D}{D_0} \quad (17)$$

$$k^* = k/C_0 \quad (18)$$

To facilitate the numerical calculation of the diffusion equation and boundary conditions, a new variable is introduced to fix the moving boundary:

$$\xi = \frac{x}{h(t)} \quad (19)$$

The dimensionless form of the governing equation (eq 3) thus becomes

$$\frac{\partial C^*}{\partial t^*} = \frac{\xi}{h^*(t^*)} \frac{dh^*(t^*)}{dt^*} \frac{\partial C^*}{\partial \xi} + \frac{1}{h^*(t^*)^2} \frac{\partial}{\partial \xi} \left( D^* \frac{\partial C^*}{\partial \xi} \right) \quad (20)$$

The dimensionless initial and boundary conditions are

$$C^* = 1 \quad t^* = 0 \quad \xi = 0 \rightarrow 1 \quad (21)$$



$$D^* \frac{\partial C^*}{\partial \xi} = 0 \quad \xi = 0 \quad (22)$$

$$-D^* \left( \frac{\partial C^*}{\partial \xi} \right)_{\xi=1} - C^*|_{\xi=1} h^*(t^*) \frac{dh^*(t^*)}{dt^*} = \alpha h^*(t^*) (C^*|_{\xi=1} - C_{\infty}^*) = Bi h^*(t^*) (C^*|_{\xi=1} - C_{\infty}^*) \quad (23)$$

where  $Bi$  is the Biot number,<sup>27,70</sup> which represents the ratio of the internal to external mass transfer resistance as defined below:

$$Bi = \frac{\alpha L_0}{D_0} \quad (24)$$

The dimensionless governing equation (eq 20), together with the dimensionless initial condition (eq 21) and boundary conditions (eqs 22 and 23), has been solved numerically (so as to fit the experimental data reported here) using  $D = 6 \times 10^{-10} \exp(-0.2/C^*)$  (m<sup>2</sup>/s) and the  $\alpha$  values which are listed in Table 3. The fittings are more sensitive to the  $\alpha$  values than to the  $D_0$  and  $k$  values. The model results on water loss shown in Figure 8a compare well to the experimental data. The numerical results also capture the film thickness evolution as shown in Figure 8b. The water distributions in the film at different times during drying at 38% RH obtained from the numerical solution are shown in Figure 9. The hydrogel film shrank significantly at the beginning of the drying process. The water concentration profiles are rather flat. However, at the later stage of the drying process, the water distribution profiles become steeper in the vicinity of the film–air boundary, which indicates an increase of the diffusion effects over the evaporation effects.

**Table 3. Constant ( $\alpha$ ) in the Film–Air Interface Boundary Condition in Pluronic P105 Hydrogels ( $L_0 = 5$  mm)**

	RH (%)					
	11	38	58	75	85	94
$\alpha$ , m/s	$18 \times 10^{-9}$	$11 \times 10^{-9}$	$8.5 \times 10^{-9}$	$7.5 \times 10^{-9}$	$5.8 \times 10^{-9}$	$3.9 \times 10^{-9}$

**Water Diffusion Coefficient.** The diffusion coefficient of water in PEO–PPO–PEO block copolymer hydrogels has been shown to depend on the block copolymer PEO/PPO composition and molecular weight and on the block copolymer concentration and temperature.<sup>41,71</sup> In particular, the diffusion coefficient of water in Pluronic P105 hydrogels was found to decrease exponentially from  $3 \times 10^{-10}$  to  $5 \times 10^{-12}$  m<sup>2</sup>/s with an increase of block copolymer concentration in the range 25–90 wt %.<sup>71</sup> The water diffusion coefficient resulting from the expression used to fit the experimental data,  $D = 6 \times 10^{-10} \exp(-0.2/C^*)$  (m<sup>2</sup>/s), is plotted in Figure 10 as a function of water concentration. In the micellar cubic and hexagonal phases of Pluronic P105 hydrogel, the values used in the model fittings change slowly and are in the same order of magnitude as the experimental values (also shown in

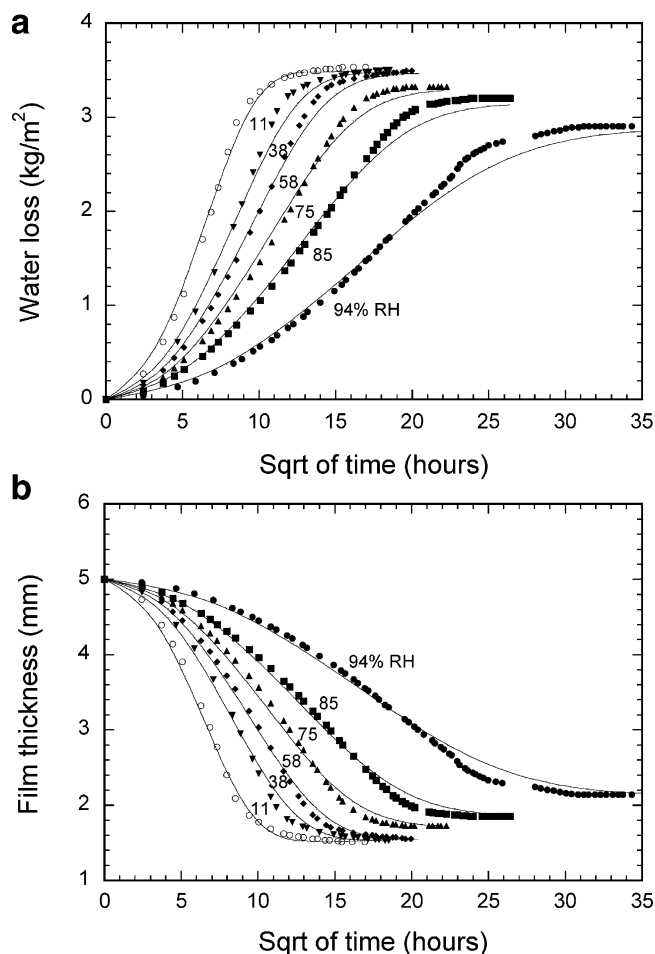


**Figure 8.** (a) Water loss per unit area vs square root of drying time at different relative humidities for Pluronic P105 hydrogels; (b) hydrogel film thickness vs square root of drying time at different relative humidities. The symbols denote the same RH conditions as in Figure 3a. Solid lines shown in the figures are results from model fittings.

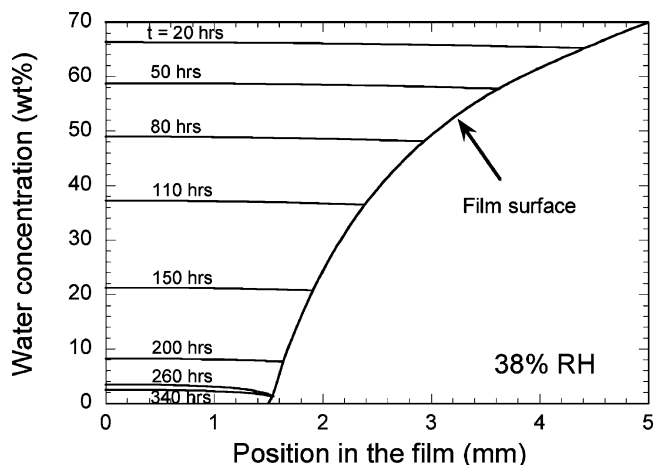


**Figure 9.** Water distribution at different times in the drying of Pluronic P105 hydrogel film at 38% RH when the initial film thickness is 5 mm and the initial block copolymer concentration is 30 wt %.

(69) Ion, L.; Vergnaud, J. M. Process of Drying a Polymeric Paint by Diffusion-Evaporation and Shrinkage. Determination of the Concentration-Dependent Diffusivity. *Polym. Testing* **1995**, *14*, 479–487.

(70) Cairncross, R. A.; Durning, C. J. A Model for Drying of Viscoelastic Polymer Coatings. *AIChE J.* **1996**, *42*, 2415–2425.

(71) Yang, L. Microstructure, Dynamics, and Applications of Solvated Amphiphilic Block Copolymers. Doctor of Philosophy Dissertation, University at Buffalo, Buffalo, NY, Sep 2000.

Figure 10). In the higher block copolymer concentration region, the water diffusion coefficient decreases quickly. In the lamellar phase, the experimental data are about 2 orders of magnitude lower than the value obtained from the model fitting. The water self-diffusion coefficient in Pluronic F127 aqueous solutions and gels was found from

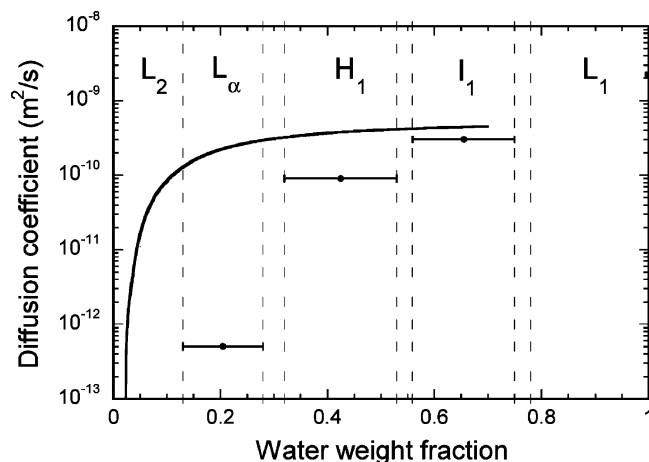


**Figure 10.** Water diffusion coefficient in Pluronic P105 hydrogel at 24 °C. Solid line,  $D = 6 \times 10^{-10} \exp(-0.2/C^*)$  ( $\text{m}^2/\text{s}$ ); ●, experimental results for Pluronic P105 from ref 71; ■, water self-diffusion coefficient in pure water [ref 72]. The error bars used for the experimental values indicate that these values are averaged over the composition range of a given phase.

pulsed field gradient spin-echo (PFGSE) NMR to decrease monotonically with increasing block copolymer concentration in the range 1–40 wt %, <sup>49</sup> which is consistent with our findings. When the Pluronic F127 concentration was 40 wt %, the water self-diffusion, about  $1.1 \times 10^{-9} \text{ m}^2/\text{s}$  at 27 °C,<sup>49</sup> was half of the self-diffusion coefficient of neat water,  $2.23 \times 10^{-9} \text{ m}^2/\text{s}$  at 25 °C.<sup>72</sup> The reduction of the water self-diffusion coefficient with increase in block polymer concentration can be explained in the context of the “obstruction effect” caused by the self-assembled structures (i.e., the part of the volume occupied by the PPO-rich domains is not readily accessible to water) and the “two-site model” which considers the hydration effect (i.e., the mobility of water molecules in the vicinity of PEO is slower than that in the bulk).<sup>50,71</sup>

**Proportionality Constant ( $\alpha$ ) in the Boundary Condition.** The proportionality constant  $\alpha$  was determined using the above model at various air RH conditions.  $\alpha$  increases linearly from 3.9 to  $18 \times 10^{-9} \text{ m/s}$  with a decrease of RH at a given film thickness (see Table 3). As we mentioned earlier, the drying in stage I is controlled (limited) by the outside air conditions rather than the diffusion in the hydrogel. The linear correlation between the  $\alpha$  values and the RH validates this supposition. The  $\alpha$  values reported here are very similar to those obtained (as a control experiment in our study) from the evaporation rate of pure water under the same drying conditions.

**Effect of Initial Film Thickness.** Film thickness is an important parameter that can be used in the dryer design and drying process optimization. Figure 11 shows the effect of film thickness on the water weight loss during the drying course of Pluronic P105 hydrogel films. The two-stage drying mechanism is maintained when the film thickness is changed; however, the drying time is greatly shortened when a lower film thickness is used. For example, when the film thickness is reduced from 5 to 1 mm, the drying time needed for achieving the removal of over 99.5% of total water is reduced from 410 to 87 h at 58% RH.

When the model used to fit the experimental results represents reality well, the water diffusion coefficient and constants ( $\alpha$ ) should be the same even if the film thickness is changed. The water diffusion model has been used to

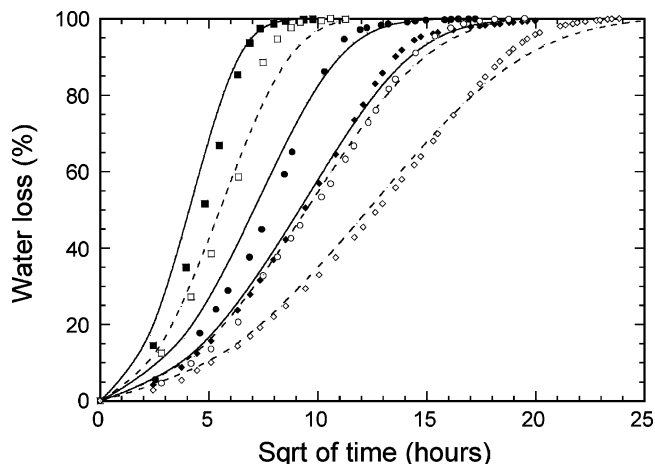


**Figure 11.** Initial film thickness effect on the drying kinetics of Pluronic P105 hydrogel film at two different relative humidities. The lines are the numerical predictions using the water diffusion model. Solid line, 58% RH; dashed line, 85% RH. The solid symbols are experimental results at 58% RH for the following film thicknesses: ■, 1 mm; ●, 3 mm; ◆, 5 mm. The empty symbols represent the corresponding film thickness at 85% RH.

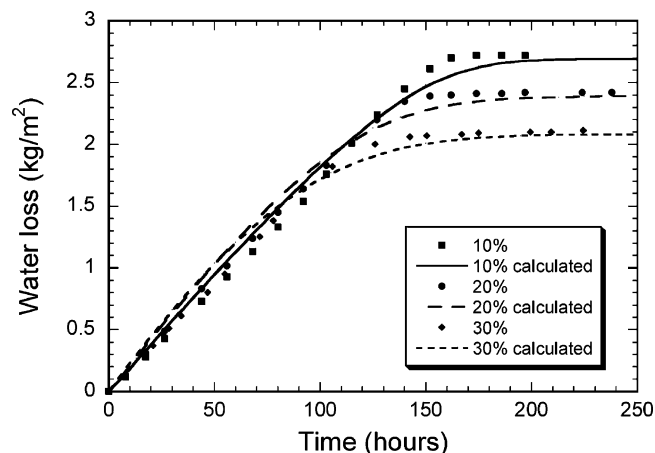


**Figure 12.** Initial water content effect on the drying kinetics of Pluronic P105 hydrogel film at 58% RH (initial film thickness of 3 mm). The lines are the numerical predictions using the water diffusion model.

fit the experimental data at different film thicknesses, and the fitting results are shown in Figure 11. Indeed, the model adequately fits the data at different film thicknesses with the same diffusion coefficient and constant ( $\alpha$ ). This means that the film thickness has no effect on the constant  $\alpha$ . So, our experimental results and diffusion model are consistent, and we can use the water diffusion coefficient  $D$  and constant  $\alpha$  obtained from fitting our experimental data to predict drying kinetics at different film thicknesses.

**Effect of Initial Solvent Concentration.** Initial solvent concentration (or polymer content) is another parameter that often varies in various applications. To access the effect of initial water content on the drying course of Pluronic P105 hydrogels, three different initial concentrations were examined at 58% RH: 10, 20, and 30 wt % Pluronic P105 (initial film thickness of 3 mm); the results are shown in Figure 12. An increase of the initial water content elongates the period of both stage I and the total drying course. This is because there is more free water in the Pluronic solution/gel initially. However, the water loss data in stage I drying of Pluronic hydrogels overlap for the three different initial solvent conditions considered here, indicating that the same mechanism is

(72) Gillen, K. T.; Douglas, D. C.; Hoch, J. R. Self-Diffusion in Liquid Water to -31 °C. *J. Chem. Phys.* **1972**, *57*, 5117–5119.

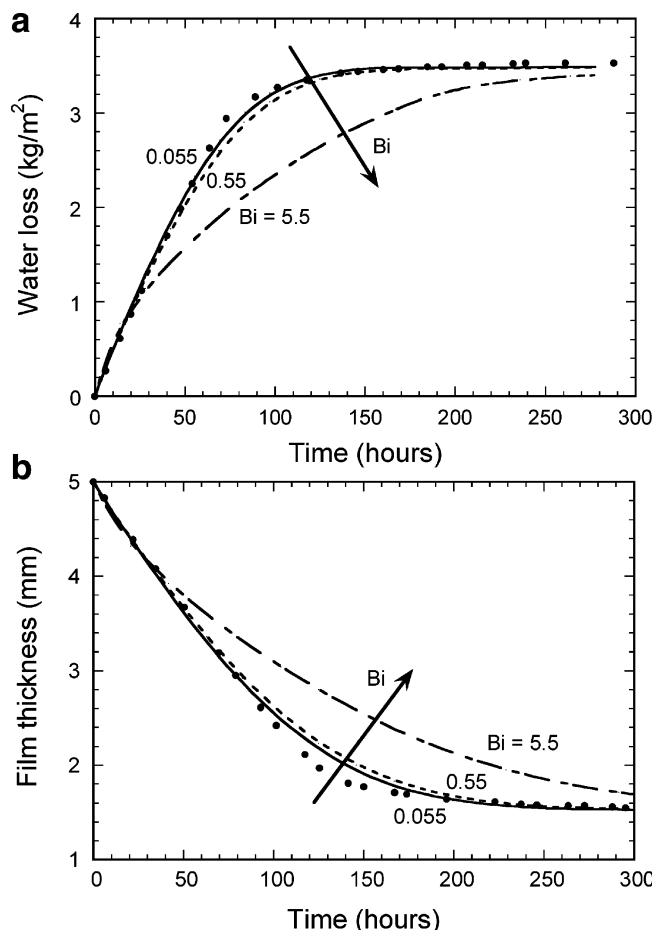


**Figure 13.** Effect of Biot number ( $Bi$ ) on (a) water loss ( $\text{kg/m}^2$ ) and (b) film thickness of Pluronic P105 hydrogel film at 38% RH when the initial film thickness is 5 mm and the initial block copolymer concentration is 30 wt %:  $\bullet$ , experimental results; solid and dashed lines, modeling results at different Biot numbers.

effective. The solid and dashed lines shown in Figure 12 are the results calculated from the models discussed above.

**Parametric Analysis. Biot Number,  $Bi$ .** The Biot number represents the internal/external mass transfer resistance. When  $Bi \ll 1$ , drying is mainly limited by the water evaporation (external resistance); when  $Bi \gg 1$ , drying is mainly determined by the water diffusion in the hydrogel film (internal resistance); and when  $Bi \approx 1$ , the drying process is limited by both evaporation and diffusion.<sup>27,70</sup> If the internal resistance, i.e., the water diffusion coefficient ( $D$ ), remains the same, an increase of the constant  $\alpha$  will increase the Biot number, correspondingly increasing the drying rate. This effect is indicated in the water loss vs drying time curves in Figure 2b, in which the water diffusion coefficient in the PEO-PPO-PEO block copolymer hydrogels is the same for all the air RH conditions, while increasing the Biot number (correspondingly  $\alpha$ ) can increase the drying rate. On the other hand, if the external resistance (i.e., mass transfer coefficient) remains the same, increasing the Biot number will decrease the drying rate. Figure 13a shows the effect of increasing Biot number on the rate of water loss per area in the drying of Pluronic P105 hydrogel at 38% RH, predicted from eq 20 with the following parameters:  $\alpha = 1.1 \times 10^{-8} \text{ m/s}$ ;  $L_0 = 0.005 \text{ m}$ ;  $D_0 = 1.0 \times 10^{-9} \text{ m}^2/\text{s}$  (for  $Bi = 0.055$ ),  $1.0 \times 10^{-10} \text{ m}^2/\text{s}$  ( $Bi = 0.55$ ), and  $1.0 \times 10^{-11} \text{ m}^2/\text{s}$  ( $Bi = 5.5$ ). As indicated in the figure, when the Biot number is relatively small, for example,  $Bi \leq 0.055$ , the magnitude of the Biot number has little effect on the drying

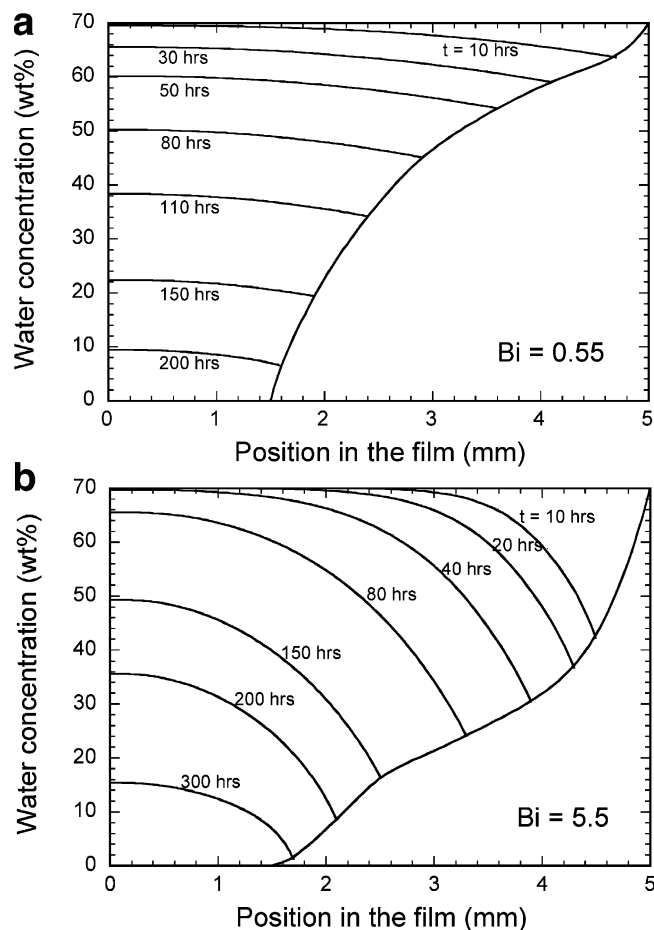


**Figure 14.** Predicted water distribution in the Pluronic P105 hydrogel film at 38% RH (the initial film thickness is 5 mm and the initial block copolymer concentration is 30 wt %) when (a)  $Bi = 0.55$  and (b)  $Bi = 5.5$  (for a comparison,  $Bi = 0.09$  for the conditions that are used to calculate the water distribution shown in Figure 9).

rate and the drying is limited by the constant  $\alpha$  (this is also reflected in the rather flat water distribution profiles shown in Figure 9). However, when  $Bi \geq 0.55$ , increasing the Biot number has great effect on the drying rate, the film thickness (see Figure 13b), and the water distribution in the hydrogel (see Figure 14a,b). For example, when  $Bi$  is 5.5, there is great concentration gradient in the hydrogel film as shown in Figure 14b, even in the initial stage of the drying process, indicating that the drying is limited by diffusion in the film at these conditions. And the film thickness change in these conditions (Figure 13b) is less compared to that at smaller Biot number conditions.

**Airflow.** In practical processes, e.g., in an industrial dryer, not only the air RH but also the airflow velocity can be utilized to alter the drying rate and drying time course. Increasing the airflow velocity has a similar effect as reducing the air RH (increasing  $\alpha$ ), since high airflow velocity increases the mass transfer of solvent in the air and thus decreases the external mass transfer resistance (correspondingly, increasing the Biot number) and shortens the drying time. Croll<sup>6</sup> observed that when the air speed was increased from relatively small (0.15 m/s) to 1.8 m/s, the water evaporation rate of a commercial latex paint increased 2.5-fold, from  $3.6 \times 10^{-2}$  to  $8.9 \times 10^{-2} \text{ g/(m}^2 \text{ s)}$  at 22 °C and 50% RH. Etemad and co-workers<sup>48</sup> observed that the drying rate of latex films formed by poly(vinyl acetate) doubled from 0.33 to 0.67  $\text{g/(m}^2 \text{ s)}$  when the air velocity doubled from 0.55 to 1.1 m/s. Saure et al.<sup>10</sup> studied the drying of poly(vinyl acetate) in organic solvents



such as methanol or benzene and found that the drying rate increased 6–7-fold when the air velocity increased from 0.25 to 30 m/s. However, optimum conditions must be obtained for the drying process because very high airflow velocity may induce the cracking of coating films and/or bubble formation within the film, which is deteriorative to the coating films.<sup>46</sup> In addition, increasing the airflow velocity normally does not change the drying rate when the solvent concentration is relatively low and the drying is diffusion-limited. In our drying experiments, there is no airflow imposed and the drying is limited by the water evaporation in stage I. As discussed earlier (see Time Evolution of Water Loss), decreasing the air RH from 94% to 11% can increase the drying rate by about 8-fold. The introducing of airflow and the increase of airflow velocity have great effect on the drying rate, as mentioned above, as much as a 6–7-fold increase when the airflow increases to high velocity. So it is expected that the drying rate will be increased greatly and the drying time will be appreciably shortened with the introduction of airflow and with the increase of the airflow velocity in the drying of PEO–PPO–PEO block copolymer hydrogels if the air RH remains unchanged.

**Temperature.** Temperature is another important parameter for the drying of polymer or gel films. The change of temperature may have two effects on the drying of PEO–PPO–PEO block copolymer hydrogels. First, increasing the temperature increases the solvent diffusion coefficient in the polymer solutions, thus increasing the drying rate. The diffusion coefficient is typically an exponential function of temperature as shown in eq 25:<sup>5,30,46,69</sup>

$$D = D_0 \exp\left(-\frac{E}{RT}\right) \quad (25)$$

where  $E$  is the activation energy of diffusion, usually 3–5 kcal/mol.<sup>46</sup> In our study, isothermal conditions were assumed when modeling the drying process of block copolymer hydrogel films. Assuming an activation energy value  $E = 4$  kcal/mol in eq 25, the water diffusion coefficient is expected to increase by a factor of about 1.7 when the temperature increases from 24 to 50 °C. As we discussed earlier, the drying rate in stage I is mainly determined by the outside air conditions, so this 1.7-fold change in diffusion coefficient may not change the drying rate appreciably in the drying of PEO–PPO–PEO block copolymer hydrogels. However, the (equilibrium) phase behavior of the block copolymer in water may change when the temperature is over 40 °C; for example, the semi-crystalline structures formed by the PEO blocks of the block copolymers will melt (amorphous state), which can dramatically change the equilibrium concentration of PEO–PPO–PEO block copolymer hydrogels (as discussed earlier in the context of Figure 7). Although this phase behavior change (correspondingly equilibrium concentration) may not change the drying mechanism in stage I, the drying rate in stage II and the total time course may be altered greatly.

Second, the water vapor pressure will increase with an increase of temperature. For example, the water vapor pressure increases about 4-fold from 0.0317 to 0.1234 bar when the temperature changes from 25 to 50 °C.<sup>73</sup> As observed by Beverley et al.,<sup>53</sup> the evaporation rate of water is proportional to the water vapor pressure at fixed temperature. So the evaporation rate of water will increase greatly at higher water vapor pressure (i.e., a bigger difference between the water vapor pressure in the liquid/gel and that in the bulk air) if the other conditions remain the same. For the PEO–PPO–PEO block copolymer hydrogels examined here, the drying rate in stage I increases linearly with a decrease of the air RH (lower RH corresponds to a bigger water vapor pressure difference between the film surface and the bulk air, as shown in Figure 3b). So the drying rate of Pluronic hydrogels will increase greatly with an increase of temperature.

## Conclusions

The drying of films formed by Pluronic poly(ethylene oxide)–poly(propylene oxide) block copolymer hydrogels is investigated at various air RH conditions covering the range from 11% to 94%. Parameters affecting the drying process, such as the air RH, block copolymer molecular weight and PEO/PPO composition, initial film thickness, and initial water content in the hydrogel, have been investigated and are reported here.

Two regimes can be distinguished in the drying process, constant drying rate (stage I) and falling drying rate (stage II). The drying rate in stage I increases linearly with a decrease of the RH. A decrease of the initial film thickness or a decrease of initial water content shortens the drying time, but the same drying mechanism is maintained.

The results indicate that the hydration level in PEO–PPO block copolymer hydrogels plays an important role in determining the drying rate, while the type of self-assembled structure formed by the block copolymers may not have appreciable effect on the drying rate. Semicrystalline structures formed by PEO blocks at low water contents affect significantly the stage II drying.

A model for one-dimensional water diffusion is used to fit the experimental drying results at different RH, initial film thickness, and initial water content conditions. The model accounts for the shrinkage of the film during drying and for a water diffusion coefficient that is a function of the water concentration in the film. For the experimental conditions considered here, the Biot number ( $Bi$ ) is less than unity and the drying is mainly limited by evaporation at the film surface. The diffusion model is used to obtain information for cases where  $Bi > 1$ .

**Acknowledgment.** Financial support to P.A. from the National Science Foundation (CTS-9875848/CAREER and CTS-0124848/TSE) is greatly appreciated.

LA0495130

(73) Felder, R. M.; Rousseau, R. W. *Elementary Principles of Chemical Processes*, 3rd ed.; John Wiley & Sons: New York, 2000.